Arabian Journal of Chemistry (2020) 13, 7160–7169

King Saud University

Arabian Journal of Chemistry

www.ksu.edu.sa
www.sciencedirect.com

ORIGINAL ARTICLE

Development of nano-tricalcium phosphate/polycaprolactone/platelet-rich plasma biocomposite for bone defect regeneration

Fan Wang [a,1], Yanqing Guo [b,1], Ruju Lv [c], Wenjuan Xu [d], Wen Wang [e,*]

[a] *Department of Orthopedics and Trauma, Shandong Provincial Qianfoshan Hospital, Shandong University, Jinan, Shandong Province 250014, China*
[b] *Department of Orthopaedics, Weihai Municipal Hospital, Weihai, Shandong Province 264200, China*
[c] *Shandong WEGO New Life Medical Devices CO.,LTD, Weihai, Shandong Province 264200, China*
[d] *Department of Neurology, Shandong Provincial Qianfoshan Hospital, The First Hospital Affiliated with Shandong First Medical University, Jinan, Shandong Province 250014, China*
[e] *Department of Orthopedics and Trauma, Shandong Provincial Qianfoshan Hospital, The First Hospital Affiliated with Shandong First Medical University, Jinan, Shandong Province 250014, China*

Received 3 June 2020; accepted 30 July 2020
Available online 6 August 2020

KEYWORDS

Biocomposite;
Bone regeneration;
Platelet-rich plasma;
Tricalcium phosphate

Abstract Nano-tricalcium phosphate (n-TCP) is an osteoconductive substance which, like polycaprolactone (PCL), has been used for clinical purposes for many years; It has now been licensed for a range of products for clinical and medication distribution. This research aimed to examine the effects of platelet-rich plasma on mesenchymal stem cell proliferation and osteogenic differentiation. Thus, we decided to examine the *in vitro* and *in vivo* actions of PRP-treated porous biocomposite scaffolds based on nano-tricalcium phosphate- polycaprolactone (n-TCP-PCL/PRP). The prepared samples were described utilizing FTIR, XRD, and SEM. MTT has measured the cytotoxicity of the biocomposite scaffolds. After two weeks of cell seeding, Alizarin red staining confirmed bone mineral formation by MSCs cells. Moreover, from day 4 to day 7, n-TCP-PCL/PRP biocomposite scaffold improved the expresses of bone marker genes. Platelet-rich plasma (PRP) in conjunction with nano-tricalcium phosphate- polycaprolactone (n-TCP-PCL) biocomposite scaffold is beneficial for the regeneration and stability of the freshly developed bone tissue.

* Corresponding author.
E-mail address: wangwenqfs@sina.com (W. Wang).
[1] Fan Wang and Yanqing Guo are co-first authors, they contributed equally to this work.

Peer review under responsibility of King Saud University.

ELSEVIER Production and hosting by Elsevier

1. Introduction

Bone and teeth can recover and redesign for the duration of human life. Under biological conditions, an animal skeleton stays in a condition of dynamic balance between steady, contradicting procedures of resorption of bone tissue and bone

https://doi.org/10.1016/j.arabjc.2020.07.021
1878-5352

formation (Chen et al., 2020; Murugan et al., 2018). Due to such physiological action, there is a balance between the substance of PO_4^{3-} ions and Ca^{2+} in hard tissue (Xing et al., 2020). Such regulation frameworks are the ones that have the potential for bone fracture repair (Subramanian et al., 2019). In the case of a person, around ten percent of bones should be removed within one year (Behera et al., 2020). Under some limits, where bone restoration is required, these properties enable the cohesion of the tissue and its subsequent rebuilding, the so-called remodeling, to be replicated to confirm its structure to the local circumstances. Remodeling takes place as a consequence of mechanical forces operating on the skeleton according to Delpech and Wolff 's rule (Afolabi et al., 2019).

The osteo-conducting properties of the bone mineral material mean that they can act as a micro-skeleton for bone tissue cells. A bone has also osteoinductive effects, which is to say it induces indistinct mesenchymal cells to divide into osteoblasts (Abdelrazik et al., 2019). This arises with the involvement of local articular cartilage renovating hormones, namely prostaglandins, protein growth factors, and cytokines (Shakir et al., 2018). Indeed, there are conditions in clinical practice where biochemical prospects for healing bone tissue are exhausted. There are bone lesions that are created and do not self-repair without surgical intervention which may require a very long time to heal. Bone defect development can be the product of post-traumatic changes, pathological fracture healing with pseudoarthrosis development, post-inflammatory changes, and tumor-like tumor lesions (Fernandez de Grado et al., 2018; Ho-Shui-Ling et al., 2018). In such situations, veterinary and medical orthopedics as well as surgical dentistry dealing with treatment of bone tissue lesions are faced with the necessity to repair bone defects to restore the continuity of tissue and to regain fitness (Skwarcz et al., 2019). Defect replacements may be performed, for instance, with auto by allogeneic grafts or a bone transplant maker in other cases. The above-mentioned strategies are restricted by the defect scale, the larger the defect, the more complicated the treatment is to treat. The clinical history indicates that while autogenic grafts typically heal well in the region of the injury, this cycle is also unreliable in the case of allogeneic grafts and bone replacements (Carlo et al., 2020). This idea prompted efforts to search for methods to improve bone replacement osseointegration.

Human bone is a natural substance composed of organic structures such as collagen and extracellular matrix (ECM) linked to glycoprotein and ceramics with calcium phosphate (Ventura et al., 2020). To minimize its relative degradation drawbacks, we experimented with the use of tricalcium phosphate (TCP) as an additive to see how it would affect the polycaprolactone (PCL) decay rate. Tricalcium phosphate is a bioceramic substance commonly used for bone tissue regeneration; it has a chemical structure close to the naturally occurring hydroxyapatite in hard tissue and has been widely used as a bone grafting medium (Zheng et al., 2019; Guiry, 2019; Wright et al., 2019). While TCP has numerous favorable features that suggest its medical usage, it also has limitations that have proved troublesome. For instance, shipping to the correct location is difficult, because it is difficult to compress sufficiently as it is fairly fragile. Throughout recent years, attempts have been made to address these drawbacks, contributing to the usage of some polymers which have the potential to strengthen TCP handling properties (Tian et al., 2019; Wang et al., 2019). For this analysis PCL was selected. Due to its cost-effectiveness, longevity, outstanding biocompatibility and biodegradability, PCL has already been licensed for a range of medical and drug delivery systems and is already commonly used for tissue recovery. Throughout the human body, PCL dissolves with no adverse effects over a while; it typically requires from six months and two years and decay throughout *Vivo*, based on its molecular weight. PCL is good mechanical strength and low biodegradability brings numerous benefits to PCL-based biomaterials for use in long-term hard regenerative medicine. Nevertheless, biomaterials and composite materials based on PCL do have certain drawbacks due to their slow pace of degradation and lack of bioavailability, thus limiting their use in hard regenerative medicine (Didekhani, et al., 2020). Surmenev et al. (2019) have studied scaffolds with Sr-HA or silicate containing PCL biocomposite are believed to hold promise for bone tissue regeneration as compared to scaffolds containing pure HA. In this way, Melnik et al. (2019) investigated The hybrid PCL/SrHA scaffolds revealed increased wet ability compared with pure PCL scaffolds that promoted the penetration of PBS into the scaffolds and increased their degradation rate *in vitro*. Many improvements would need to be learned to solve such limits.

The usage of autogenous fibrin glue and platelet-rich plasma, respectively, in mandibular production, was first described by Tayapongsak et al. (1994) and subsequently by Marx et al. (1998). Platelets may be a source of the aforementioned signaling molecules, and others (Fuentes et al., 2019). While releasing factors involved in coagulation and fibrinolysis, proteolytic enzymes, and antibacterial proteins, thrombocytes are a source of cytokines that aid in the process of regeneration of bone tissues (Ramirez et al., 2019). Platelet-rich plasma is used for a broad variety of purposes both in animal and clinical medicine. Throughout clinical research, this is used for the diagnosis of soft tissue disease, especially entesopathy and tendinopathy, in accepted surgical procedures (Evenski et al., 2019). Nevertheless, it may also be used individually or as a form of adjuvant therapy in the care of bone tissue, cartilage, soft tissue fractures, cosmetic medicine, and dentistry associated pathologies. However, its efficacy is often doubtful in other signs (Smith et al., 2019). Relatively further questions arose regarding its efficacy in managing an injury to the bone.

Concerning these factors, this study aimed to produce a biocomposite scaffold of appropriate osteoconductivity; thus, for bone tissue engineering applications the authors built a biocomposite made of n-TCP-PCL/PRP scaffolds.

2. Materials and method

2.1. Preparation of n-TCP-PCL biocomposite

n-TCP is prepared with $Ca(OH)_2$ and H_3PO_4 as discussed in past studies (Sarkar et al., 2019) utilizing wet precipitation path. The TCP-PCL biocomposite fabric utilized in this investigation was acquired by employ a hybrid-defoaming blender to combine TCP and PCL with biocomposite weight proportion of 50:50 for 15 min, after which the combination was ball-milled in alcohol using ethyl liquor employing a centrifugal ball process for 4 h. Then the TCP-PCL biocomposite was

formed into a Teflon mold and put for 45 min in a 100 °C hot air oven. All chemicals were purchased from Sigma-Aldrich (Shanghai, China) and used without further purification except when mentioned specifically.

2.2. Preparation of n-TCP-PCL/PRP biocomposite

At room temperature, the preparation of activated PRP 50 mL of human plasma was centrifuged for 10 min and the supernatant was discarded. Activated PRP was fabricated for every 20 mL of PRP solution by adding 500 μL of $CaCl_2$ 10% w/v (Sadeghinia et al., 2019; Tang et al., 2019). The sterilized n-TCP-PCL composite with UV radiation is submerged in the PRP mixture and then incubated at RT in a vacuum oven to catch air bubbles and allow homogeneous PRP diffusion within the biocomposite.

2.3. Characterization

2.3.1. Physicochemical analysis

SEM (SEM, TM-4000, Hitachi, Tokyo, Japan) was used to examine the structure and pore size of prepared scaffolds. As described elsewhere, the physicochemical characterization of the scaffolds was performed through porosity, swells, flow rate and pore size analysis. X-ray diffraction was used to analyze the composition of the n-TCP and biocomposite scaffold (Rigaku D/MAX-RB, Japan).

2.3.2. Biocompatibility assay

Cell proliferation was assessed by the MTT test. Based on this assess, livelihood cells can in the attendance of effective mitochondria reduce the MTT substrate to dark blue formazan and thus are a precise cell proliferation determine for a culture. To experiment, 50.000 cells/well are seeded in and grown in a 96-well system and incubated for one, five and fourteen days at 37 °C. After that time, the specimen was taken away to 96-well platforms and MTT included to them at 37 °C for 5 h before the incubation processes were completed. The MTT solution has been separated and the violet formosan crystals dissolved with DMSO.

2.3.3. Osteogenic differentiation

Alkaline phosphatase (ALP) activity was used to study the osteogenic differentiation of mesenchymal stem cells seeded on biocomposite. The staining of Alizarin Red Staining (ARS) was performed to determine osseous mineralization. ARS staining is commonly used to test cell deposits of high calcium in culture content (Gregory et al., 2004).

2.3.4. Gene expression

A quantitative continuous invert translation polymerase chain response strategy was utilized. In the wake of refined in the osteogenic mode for 4 and 14 days, the all-out cell RNA of cells were separated by methods for TRIzol reagent as indicated by the producer's convention. Turn around interpreted to cDNA was completed utilizing the cDNA Synthesis Kit. The focus and nature of disengaged RNA were resolved dependent on OD esteem 260/280 proportion, and its quality was evaluated on agarose gel electrophoresis. Following converse interpretation, cDNA was measured on a constant PCR discovery framework. Relative articulation for each target quality was determined to utilize the $-2\Delta\Delta Ct$ strategy.

2.3.5. In vivo analysis

All experiments involving the use of animals were carried out following the Institutional Animal Care and Use Committee of the Department of Orthopedics and Trauma, Shandong Provincial Qianfoshan Hospital, Shandong University. Hares were set in the prostrate position and the lower arms were shaved, prepared, and hung for an aseptic medical procedure. A 4 cm, the dorsomedial entry point was made, and the tissue overlying the mid-shaft of the span was carefully dismembered. A 2 cm fragment of the sweep and overlying periosteum was respected utilizing an electrical saw, and a sheet of dialysis film was put on the presented ulna to keep bone development from the ulnar exterior. The biocomposite was pressed inside the imperfection. The encompassing muscles and belt were fixed accurately utilizing absorbable polyglactin sutures to keep unites from relocating out of the endless supply of the creatures. The skin was shut with persistent running nylon sutures. Postoperatively, hares were infused intramuscularly with gentamicin and they were permitted to walk uninhibitedly in their confines. Histological assessment for desorption of the joined bone granule, the level of fresh bone development, the development design including proof of early redesigning and any unfriendly incendiary reaction was performed utilizing an Olympus BX51 microscope instrument.

2.4. Statistical analysis

The data were obtained at least in triplicate ($n = 3$), averaged and expressed as the mean ± standard deviation (SD). Computation of statistical signifcance between four types of samples was analyzed using one-way ANOVA with a post hoc Tukey's HSD test provided by the Statsmodels module for the Python programming language.

3. Results and discussion

3.1. Physicochemical characterization

The FTIR spectra in Fig. 1A demonstrated PO_4^{3-} groups at 555 and 606 cm^{-1} and as well as 1021 and 1119 cm^{-1} in the two materials, which are normal for n-TCP. The wide adsorption tops around 1090 cm^{-1} in biocomposite are ascribed to the P—O extending vibration methods of the PO_4^{3-} groups (Viswanathan et al., 2019). The peaks at 560 and 605 cm^{-1} are credited to the P—O bowing vibration of crystalline PO_4^{3-} bunches in n-TCP crystals. The biocomposite scaffolds FTIR spectra (Fig. 1A) display the major polycaprolactone peaks as follows: 2886 cm^{-1} and 2986 cm^{-1} (symmetric CH_2 and asymmetric CH_2 stretching vibration, respectively), 1787 cm^{-1} (C═O stretching), 1280 cm^{-1} (C—C and C═O stretching), and 1157 cm^{-1} (C═O and C—C stretching in the amorphous phase) (Hirose et al., 2002; Elzein et al., 2004). The n-TCP spectra displayed typical peaks at 622 cm^{-1} (OH— group libration), at 605 and 567 cm^{-1} (corresponding to phosphate group bending vibrations). Regardless of the overlap with the apex of the stretching vibration C═O, the high peak at 1019 cm^{-1} assigned to the phosphate group

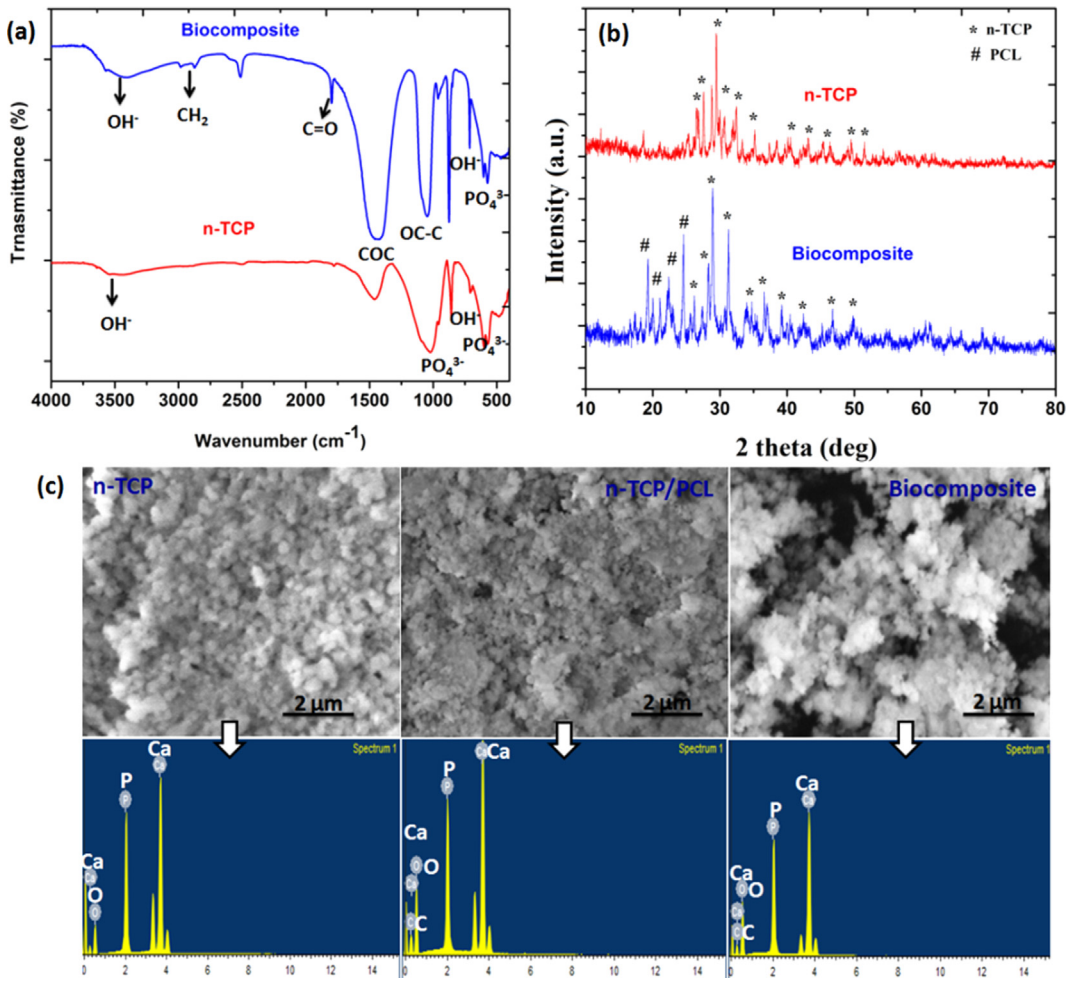

Fig. 1 (a) FTIR spectrum; (b) XRD patterns of n-TCP and biocomposites; (c) SEM-EDX images of prepared samples.

present in n-TCP was not observed in the biocomposite scaffold spectra (Melnik et al., 2019).

All prepared samples showed the typical diffraction peaks of TCP crystal (JCPDS 090169) (Maheshwari et al., 2018) (Fig. 1B). The X-ray diffraction patterns had diffraction plane (220), (111) and (110) corresponding to the 23.6°, 21.8°, and 21.4° reflection of polycaprolactone. At diffraction plane (300), (112), and (211), which were allocated 32.9°, 32.3°, and 31.5°, the most intense reflections attributable to n-TCP nanoparticles have been identified (Shkarina et al., 2018) (Fig. 1B). All peaks correlate with the reported results in strong association (Bittiger et al., 1970; Caicedo et al., 2020). The findings obtained with the FTIR and XRD spectroscopy support the effective integration of n-TCP in the PCL/PRP biocomposite system.

The morphology and pores size of the prepared biocomposite scaffolds were imaged utilizing scanning electron microscopy (Fig. 1C). All the prepared biocomposites of scaffolds were permeable with pore size in the scope of 50–500 µm. The addition of PRP didn't influence the pore size of the biocomposite scaffold. n-TCP-PCL and n-TCP-PCL/PRP biocomposites had normal porosity of 73.8 ± 5% and 81.5 ± 4% respectively, as assessed by the cyclohexane technique. Scanning electron microscopy examination of the biocomposites revealed consolidation of PRP into the scaffold network and dividers, because of which biocomposite had unpleasant surface and much grainy and permeable engineering when contrasted with n-TCP-PCL biocomposite which is having smooth dividers (Fig. 1C). Surface roughness is also established to boost cellular proliferation and distribution; the rough surface of the n-TCP-PCL biocomposite may help to improve cell attachment and diffusion (Siddiqui et al., 2020). Pore size research on scanning electron microscopy photos using image J showed that biocomposites are around 50–230 µm in macroporous pores (Zhou et al., 2017). The ideal pore size for osteoleitration was 150–500 µm respectively, proposed by Hulbert et al. (1972) and Flatley et al. (1983). The solvent convective flow describes pore-connectivity, as defined by the flow study of porous skin, and describes the capacity of porous skin to enable the transportation of blood and nutrients (Liu et al., 2019; Wang et al., 2020).

Fig. 1C represents the SEM-EDX spectra for n-TCP, n-TCP-PCL, and n-TCP-PCL/PRP, respectively. The EDX spectra described the peaks of elements Ca, P, C and O, and their qualitative abundance in n-TCP, n-TCP-PCL, and n-TCP-PCL /PRP. Based on the EDX spectra, the Ca/P weight ratio for n-TCP, n-TCP-PCL, and n-TCP-PCL/PRP was calculated and was found to be 1.52, 1.56 and 1.48, respectively; the resulting values are reliable with earlier values accounted elsewhere (Venkatesan and Kim, 2010; Donate et al., 2020). The

EDX finding in Fig. 1C reveals that during the milling phase no impurities are introduced into the biocomposites, which indicates that solid-state shear friction is a simple and effective method to distribute TCP particles through the PCL matrix.

3.2. Cell proliferation assay

The impacts of the n-TCP, n-TCP-PCL, and biocomposite (n-TCP-PCL/PRP) on the expansion and cell practicality were evaluated utilizing an MTT assay. The outcomes in Fig. 2a demonstrated that cell proliferation on various samples was comparable on day one. Cell proliferation from n-TCP-PCL and biocomposite, however, was altogether more significant than that of the control samples on all days. There was no huge contrast between the n-TCP-PCL and biocomposite in any of the examined days. On day 14, the mesenchymal stem cells presented to the n-TCP-PCL/PRP biocomposite indicated an expansion in cell multiplication in contrast with n-TCP. The results showed that PRP can positively affect the proliferation of mesenchymal stem cells (Fig. 2a). Recent literature proposes that PRP invigorates the expansion of different begetter and undifferentiated cells (Reddy et al., 2018; Hoberman et al., 2018; Fernandes and Yang, 2016).

3.3. Live/dead cell assay

To observe the cell reaction to the biocomposites, we utilized the control and PRP based biocomposites, which had comparative pore geometry. To start with, we performed live/dead cell tests utilizing mesenchymal stem cells preosteoblasts to decide cell viability on the biocomposite scaffolds. The estimation was led for a few periods (4 days, and 14 days). As presented in Fig. 2b, most cells on both the biocomposites were all around connected, multiplied, and feasible until 14 days of cell incubation. Also, the cell viability for both the biocomposites was comparative and high, showing that the biocomposite was safe biomaterials (Fig. 2b).

In contrast to the MSCs cells on the n-TCP-PCL, the loading of platelet-rich plasma on/in the biocomposite scaffolds has shown to improve stem cell feasibility. However, the n-TCP-PCL/PRP scaffolds were able to trigger the division of stem cells through endothelial and osteogenic groups, without supplying any supplements. This was confirmed by early bone indicators such as ALP and endothelial indicators such as nitric oxide and VEGF (Shamaz et al., 2015; Masoud et al., 2012; Ghasemi and Zahediasl, 2012; Bocci et al., 2001). Nonetheless, further work to establish the full differentiation of stem cells into endothelial and osteoblasts cells should be performed. Platelet-rich plasma usually has a beneficial impact on osteoblast-like cells, since it activates a combination of growth factors such as TGF-band PDGF to activate cells (Bir et al., 2009). Several kinds of research have also shown platelet-rich plasma mediated proliferation of osteoblasts by utilizing fetal bovine serum. Consequentially, owing to the involvement of signaling pathways such as VEGF and PDGF, platelet-rich plasma has shown to facilitate the development of endothelial cells and the creation of blood vessels (Kurita et al., 2011).

3.4. Mineralization assay

The osteogenic differentiation of mesenchymal stem cells seeded on n-TCP-PCL biocomposite with PRP was analyzed by alizarin red S (ARS) staining, surely understood as a late marker of osteogenesis, to determine network mineralization. Following 14 days of incubation, the concentration of ARS on the n-TCP-PCL biocomposite with PRP was essentially higher than that of different groups. In this manner, n-TCP-PCL/PRP biocomposite showed the most remarkable bone mineralization among the groups (Fig. 3a).

These findings suggested, in other terms, that the platelet-rich plasma-treated biocomposite scaffold displayed greater differentiation and mineralization than the control group. PRP includes numerous growth factors including PDGF, TGF-β1, and IGF that can stimulate regeneration of the bone (Lu et al., 2008; Marx et al., 1998). However, with both *in vitro* and *in vivo* studies, the effectiveness of platelet-rich plasma for bone tissue regeneration remains unclear (Kasten et al., 2006; Kasten et al., 2008a,b; Kasten et al., 2012). In an *in vitro* study, the differentiation and proliferation of the platelet-rich plasma-containing PCL and TCP biocomposite scaffold were better than the non-PRP group (Kasten et al., 2008a,b).

The ALP activity among of the mesenchymal stem cells incubation on n-TCP-PCL/PRP biocomposite increased essentially with correlation with the n-TCP-PCL and control samples following 2 culture weeks. This augmentation demonstrates that the mesenchymal stem cells gradually differentiate into osteoblasts (Fig. 3b). Additionally, the differentia-

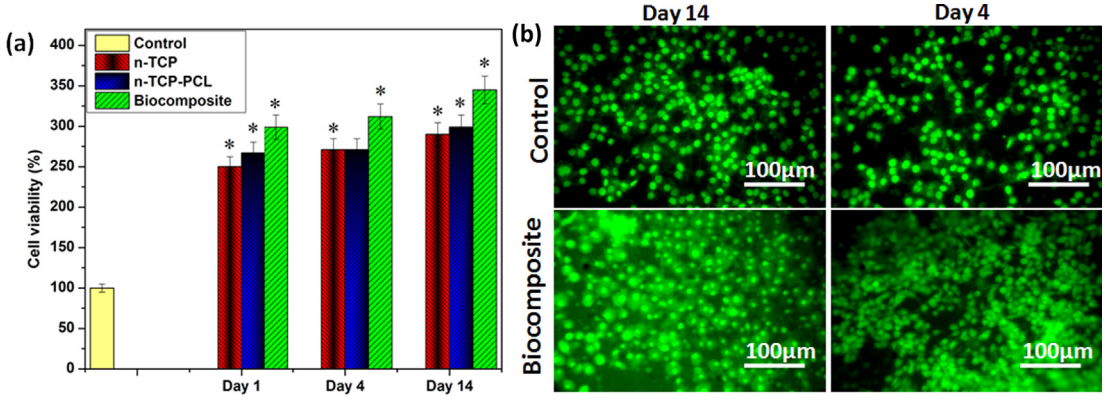

Fig. 2 (a) Cell viability (*p < 0.05); (b) Live/dead cell assay of biocomposite.

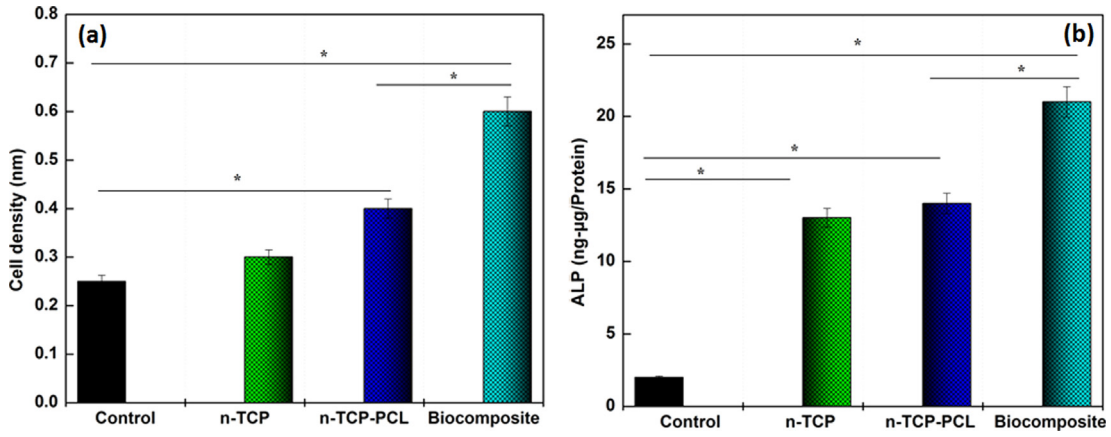

Fig. 3 (a) ALP activities and (b) osteogenic differentiation of prepared samples (*p < 0.05).

tion of the n-TCP-PCL biocomposite treated PRP was altogether higher than n-TCP-PCL and control groups. Because of the elevated rate of cell proliferation caused by the release of PRP-derived growth factors including TGF-β1 and PDGF. It is understood that the PDGF induces stem cell and osteoblast mitogenesis, which improves cell formation, and that TGF-β1 triggers preosteoblast to proliferate and grow (Blom et al., 2000; Sarkar et al., 2006). Based on the findings, we critically predicted the signaling molecules derived from PRP could promote the differentiation and proliferation of preosteoblast cells with CaP scaffold.

3.5. Gene expression

The relative gene expression of each fabricated samples contrasted with the control sample. As appeared in Fig. 4, the expression of the genes BMP2 and RUNX2 expanded in the n-TCP-PCL biocomposites that were treated with PRP in correlation with the control group on day 4. Also, the expression of all genes for the n-TCP-PCL/PRP, n-TCP-PCL, and n-TCP samples demonstrated a huge increment contrasted and control group on day 14. The gene expression BMP2 likewise indicated increment in the n-TCP-PCL/PRP samples contrasted and all group on day 14. The n-TCP-PCL group on both 4 and 14 days didn't have a huge contrast with a control group.

Osteoblast differentiation is regulated by classes of cytokines, receptors, cell proliferation, and other signal transduction (Luttrell et al., 2019). Additionally, osteogenic cells started cell division and maturation. Researchers introduced the development of specific osteoblast markers, including genes such as Runx2 and related protein mineralization processes such as ALP, collagen type I, OC, OPN, and BMP-2. In PRP-seeded biocomposite scaffolds, osteogenic-related expressions like RUNX2, OC, and BMP2 were upreguled to rates higher than in untreated biocomposite scaffolds (Kmiecik et al., 2015; Sadeghinia et al., 2019). It should be remembered that the n-TCP-PCL/PRP gene expressions were the strongest among the various classes.

3.6. Histocompatibility study

In vivo animal model examination (Fig. 5) further showed that the biocomposite advanced bone recovery and osteogenesis at the interface between the biocomposite and the imperfection. The T. blue stained segments demonstrated that new bone was available in the biocomposite implanted model following 1st month. Following 3rd month, a thick new layer of bone with osteocytes had shaped, showing incredible osseointegration between the biocomposite and the host tissue at the boundary. Though, in the n-TCP-embedded model, there was a prevalence of connective stringy tissue between the biocomposite and the host ligaments at both times focuses. Constrained fresh bone was framed following 3rd¯month implantation. The histocompatibility outcomes showed mineralized osteoid in the biocomposite-embedded models at the 1st-month post-medical procedure, which commanded at the interface between the host tissue and the embedded biocomposite following 3rd month. We demonstrate that not many cells moved into the biocomposite because of the low degradability of TCP. A thick new bone layer at the interface of the local bone and the biocomposite effectively fastened the platform inside the imperfection site, and this gave burden-bearing to the local tissue. Henceforth, through in situ mineralization, we developed a bioactive n-TCP layer inside the biocomposite arrange that biodegradable polymer and PRP with its osteoconductive and osseointegrated potential and therefore brought about direct holding of the framework to the host bone and the incitement of new bone arrangement.

Many studies have shown that *in vivo* animals, calcium phosphate (CaP) scaffolds with platelet-rich plasma and stem cells have improved bone formation. On the contrary, a team of researcher's notes that PRP-CaP and TCP biocomposites have no improved osteogenic characteristics relative to PRP-free scaffolds in the animal model (Kasten et al., 2006; Kasten et al., 2008a,b; Kasten et al., 2012; El Backly et al., 2014). Sarkar et al. (2006) have stated that in the sheep model for bone regeneration there is no substantial difference between PRP specimens with or without them.

4. Conclusion

In this investigation, a bio-ceramic based scaffolds, comprising of n-TCP-PCL mixer and PRP, was fabricated utilizing ball milling. Despite the controversy over platelet-rich plasma significance for bone tissue regeneration, the findings of our *in vitro* study using preosteoblasts revealed that the platelet-

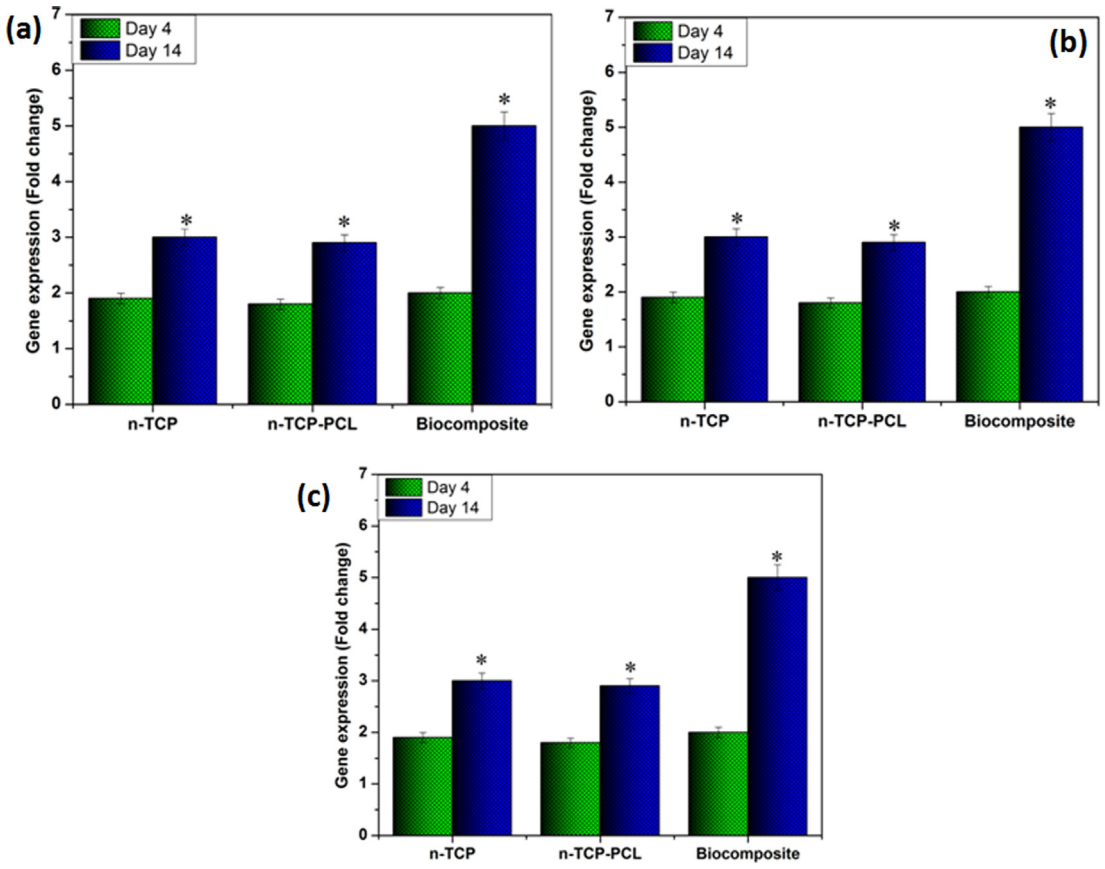

Fig. 4 Osteogenic gene expesssion in stem cell seeded on the prepared samples: (a) RUNX-2,(b) OCN, and (c) BMP2 expression at 4 and 14 days (*$p < 0.05$).

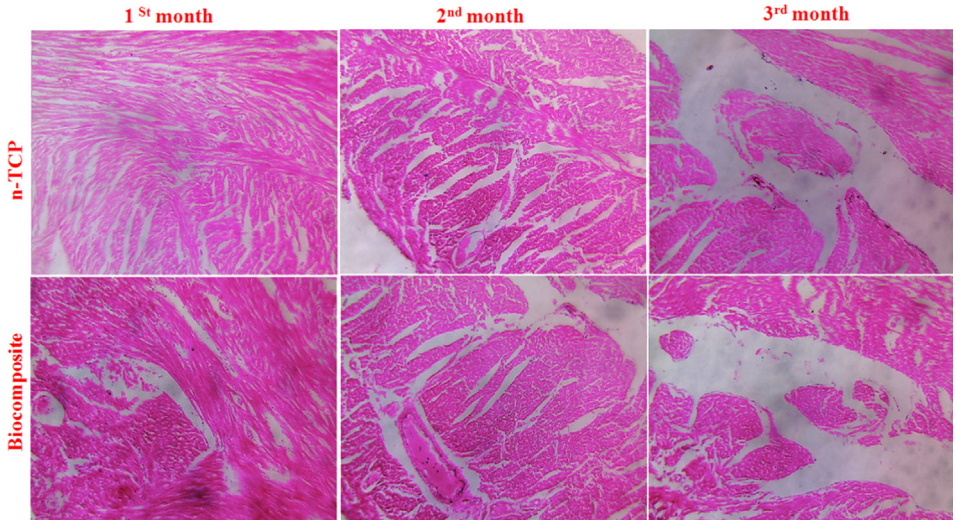

Fig. 5 Histological analyses of regenerated tissues.

rich plasma-based biocomposite scaffold cell proliferation and bone mineralization are substantially higher than those of the control. The findings suggested that in terms of cell proliferation and differentiation the continuously released platelet-rich plasma had beneficial effects on the preosteoblast cells. Based on these findings our n-TCP-PCL/PRP biocomposite scaffold can be used as an excellent biocompatible scaffold for the restoration of bone tissue. Further work on the optimum PRP-based scaffold preparation process, concentration, and frequency of application is required. Besides, considers including a more prominent number of subjects and bigger creatures ought to be performed to assess the clinical pertinence of

platelet-rich plasma. Therefore, to determine the therapeutic importance of platelet-rich plasma-based scaffold, trials covering a greater number of samples and larger species will be carried out.

Declaration of Competing Interest

The authors declare that they have no known competing financial interests or personal relationships that could have appeared to influence the work reported in this paper.

Acknowledgements

The authors are thankful to the Department of Orthopedics and Trauma, Shandong Provincial Qianfoshan Hospital, Shandong University, China for availing the needed laboratory and instrument facilities.

References

Afolabi, H.A., bin Zakaria, Z., Hashim, M.N.M., Vinayak, C.R., Shokri, A.B.A., 2019. Body Mass Index and predisposition of patients to knee osteoarthritis. Obes. Med. 16.

Abdelrazik, H., Giordano, E., Barbanti Brodano, G., Griffoni, C., De Falco, E., Pelagalli, A., 2019. Substantial overview on mesenchymal stem cell biological and physical properties as an opportunity in translational medicine. Int. J. Mol. Sci. 20, 5386.

Blom, E.J., Klein-Nulend, J., Klein, C.P.A.T., Kurashina, K., Van Waas, M.A.J., Burger, E.H., 2000. Transforming growth factor-β1 incorporated during setting in calcium phosphate cement stimulates bone cell differentiation in vitro. J. Biomed. Mater. Res.: Offic. J. Soc. Biomater. Jpn. Soc. Biomater. 50, 67–74.

Behera, D.R., Nayak, P., Rautray, T.R., 2020. Phosphatidylethanolamine impregnated Zn-HA coated on titanium for enhanced bone growth with antibacterial properties. J. King Saud Univ.-Sci. 32, 848–852.

Bittiger, H., Marchessault, R.H., Niegisch, W.D., 1970. Crystal structure of poly-ε-caprolactone. Acta Crystall. Sec B: Struct. Crystall. Crystal Chem. 26, 1923–1927.

Bir, S.C., Esaki, J., Marui, A., Yamahara, K., Tsubota, H., Ikeda, T., Sakata, R., 2009. Angiogenic properties of sustained release platelet-rich plasma: characterization in-vitro and in the ischemic hind limb of the mouse. J. Vasc. Surg. 50, 870–879.

Bocci, G., Fasciani, A., Danesi, R., Viacava, P., Genazzani, A.R., Tacca, M.D., 2001. In-vitro evidence of autocrine secretion of vascular endothelial growth factor by endothelial cells from human placental blood vessels. MHR: Basic Sci. Reprod. Med. 7, 771–777.

Carlo, B., Augusto, C., Filippo, Z., Elisa, B., Pietro, R., 2020. ACL reconstruction using a bone patellar tendon bone (BPTB) allograft or a hamstring tendon autograft (GST): a single-center comparative study. Acta Bio Medica: Atenei Parmensis 90, 109.

Caicedo, J.C., Caicedo, H.H., Ramirez-Malule, H., 2020. Structural and chemical study of β–Tricalcium phosphate-chitosan coatings. Mater. Chem. Phys. 240, 122251.

Chen, M., Zhang, H., Shan, S., Li, Y., Li, X., Peng, D., 2020. Fabrication of multiwalled carbon nanotubes/carrageenan-chitosan@ Ce and Sr substituted hydroxyapatite biocomposite coating on titanium: in vivo bone formation evaluations. J. King Saud Univ.-Sci. 32, 1175–1181.

Didekhani, R., Sohrabi, M.R., Soleimani, M., Seyedjafari, E., Hanaee-Ahvaz, H., 2020. Incorporating PCL nanofibers with oyster shell to improve osteogenic differentiation of mesenchymal stem cells. Polym. Bull. 77, 701–715.

Donate, R., Monzon, M., Ortega, Z., Wang, L., Ribeiro, V., Pestana, D., Oliveira, J.M., Reis, R.L., 2020. Comparison between calcium carbonate and β-tricalcium phosphate as additives of 3D printed scaffolds with polylactic acid matrix. J. Tissue Eng. Regener. Med. 14, 272–283.

Evenski, A.J., Stensby, J.D., Rosas, S., Emory, C.L., 2019. Diagnostic imaging and management of common intra-articular and periarticular soft tissue tumors and tumorlike conditions of the knee. J. Knee Surgery 32, 322–330.

El Backly, R.M., Zaky, S.H., Canciani, B., Saad, M.M., Eweida, A. M., Brun, F., Tromba, G., Komlev, V.S., Mastrogiacomo, M., Marei, M.K., Cancedda, R., 2014. Platelet rich plasma enhances osteoconductive properties of a hydroxyapatite-β-tricalcium phosphate scaffold (Skelite™) for late healing of critical size rabbit calvarial defects. J. Cranio-Maxillofacial Surgery 42, 70–79.

Elzein, T., Nasser-Eddine, M., Delaite, C., Bistac, S., Dumas, P., 2004. FTIR study of polycaprolactone chain organization at interfaces. J. Colloid Interface Sci. 273, 381–387.

Fernandes, G., Yang, S., 2016. Application of platelet-rich plasma with stem cells in bone and periodontal tissue engineering. Bone Res. 4, 1–21.

Fernandez de Grado, G., Keller, L., Idoux-Gillet, Y., Wagner, Q., Musset, A.M., Benkirane-Jessel, N., Bornert, F., Offner, D., 2018. Bone substitutes: a review of their characteristics, clinical use, and perspectives for large bone defects management. J. Tissue Eng. 9 (2041731418776819).

Flatley, T.J., Lynch, K.L., Benson, M., 1983. Tissue response to implants of calcium phosphate ceramic in the rabbit spine. Clin. Orthop. Related Res.® 179, 246–252.

Fuentes, E., Moore-Carrasco, R., de Andrade Paes, A.M., Trostchansky, A., 2019. Role of platelet activation and oxidative stress in the evolution of myocardial infarction. J. Cardiovasc. Pharmacol. Therap. 24, 509–520.

Ghasemi, A., Zahediasl, S., 2012. Preanalytical and analytical considerations for measuring nitric oxide metabolites in serum or plasma using the Griess method. Clin. Lab. 58, 615–624.

Guiry, E.J., 2019. Complexities of stable carbon and nitrogen isotope biogeochemistry in ancient freshwater ecosystems: implications for the study of past subsistence and environmental change. Front. Ecol. Evolut. 7, 313.

Gregory, C.A., Gunn, W.G., Peister, A., Prockop, D.J., 2004. An Alizarin red-based assay of mineralization by adherent cells in culture: comparison with cetylpyridinium chloride extraction. Anal. Biochem. 329, 77–84.

Hirose, S., Hatakeyama, T., Izuta, Y., Hatakeyama, H., 2002. TG-FTIR studies on lignin-based polycaprolactones. J. Therm. Anal. Calorim. 70, 853–860.

Hoberman, A.R., Cirino, C., McCarthy, M.B., Cote, M.P., Pauzenberger, L., Beitzel, K., Mazzocca, A.D., Dyrna, F., 2018. Bone marrow-derived mesenchymal stromal cells enhanced by platelet-rich plasma maintain adhesion to scaffolds in arthroscopic simulation. Arthrosc.: J. Arthrosc. Related Surgery 34, 872–881.

Ho-Shui-Ling, A., Bolander, J., Rustom, L.E., Johnson, A.W., Luyten, F.P., Picart, C., 2018. Bone regeneration strategies: engineered scaffolds, bioactive molecules and stem cells current stage and future perspectives. Biomaterials 180, 143–162.

Hulbert, S.F., Morrison, S.J., Klawitter, J.J., 1972. Tissue reaction to three ceramics of porous and non-porous structures. J. Biomed. Mater. Res. 6, 347–374.

Kasten, P., Vogel, J., Luginbühl, R., Niemeyer, P., Weiss, S., Schneider, S., Kramer, M., Leo, A., Richter, W., 2006. Influence of platelet-rich plasma on osteogenic differentiation of mesenchymal stem cells and ectopic bone formation in calcium phosphate ceramics. Cells Tissues Organs 183, 68–79.

Kasten, P., Vogel, J., Geiger, F., Niemeyer, P., Luginbühl, R., Szalay, K., 2008a. The effect of platelet-rich plasma on healing in critical-size long-bone defects. Biomaterials 29, 3983–3992.

Kasten, P., Vogel, J., Beyen, I., Weiss, S., Niemeyer, P., Leo, A., Lüginbuhl, R., 2008b. Effect of platelet-rich plasma on the in vitro

proliferation and osteogenic differentiation of human mesenchymal stem cells on distinct calcium phosphate scaffolds: the specific surface area makes a difference. J. Biomater. Appl. 23, 169–188.

Kasten, P., Beverungen, M., Lorenz, H., Wieland, J., Fehr, M., Geiger, F., 2012. Comparison of platelet-rich plasma and VEGF-transfected mesenchymal stem cells on vascularization and bone formation in a critical-size bone defect. Cells Tissues Organs 196, 523–533.

Kmiecik, G., Spoldi, V., Silini, A., Parolini, O., 2015. Current view on osteogenic differentiation potential of mesenchymal stromal cells derived from placental tissues. Stem Cell Rev. Rep. 11, 570–585.

Kurita, J., Miyamoto, M., Ishii, Y., Aoyama, J., Takagi, G., Naito, Z., Tabata, Y., Ochi, M., Shimizu, K., 2011. Enhanced vascularization by controlled release of platelet-rich plasma impregnated in biodegradable gelatin hydrogel. Ann. Thoracic Surgery 92, 837–844.

Liu, S., Hu, Y., Zhang, J., Bao, S., Xian, L., Dong, X., Zheng, W., Li, Y., Gao, H., Zhou, W., 2019. Bioactive and biocompatible macroporous scaffolds with tunable performances prepared based on 3D printing of the pre-crosslinked sodium alginate/hydroxyapatite hydrogel ink. Macromol. Mater. Eng. 304, 1800698.

Lu, H.H., Vo, J.M., Chin, H.S., Lin, J., Cozin, M., Tsay, R., Eisig, S., Landesberg, R., 2008. Controlled delivery of platelet-rich plasma-derived growth factors for bone formation. J. Biomed. Mater. Res. Part A: Offic. J. Soc. Biomater. Jpn. Soc. Biomater. Aust. Soc. Biomater. Korean Soc. Biomater. 86, 1128–1136.

Luttrell, L.M., Dar, M.S., Gesty-Palmer, D., El-Shewy, H.M., Robinson, K.M., Haycraft, C.J., Barth, J.L., 2019. Transcriptomic characterization of signaling pathways associated with osteoblastic differentiation of MC-3T3E1 cells. PLoS ONE 14, 0204197.

Marx, R.E., Carlson, E.R., Eichstaedt, R.M., Schimmele, S.R., Strauss, J.E., Georgeff, K.R., 1998. Platelet-rich plasma: growth factor enhancement for bone grafts. Oral Surgery Oral Med. Oral Pathol. Oral Radiol. Endodontol. 85 (6), 638–646.

Maheshwari, S.U., Govindan, K., Raja, M., Raja, A., Pravin, M.B., Kumar, S.V., 2018. Synthesis and characterization of calcium phosphate ceramic/(poly (vinyl alcohol)–polycaprolactone) bilayer nanocomposites-A bone tissue regeneration scaffold. J. Nanosci. Nanotechnol. 18, 1548–1556.

Masoud, M.S., Anwar, S.S., Afzal, M.Z., Mehmood, A., Khan, S.N., Riazuddin, S., 2012. Pre-conditioned mesenchymal stem cells ameliorate renal ischemic injury in rats by augmented survival and engraftment. J. Trans. Med. 10, 243.

Melnik, E.V., Shkarina, S.N., Ivlev, S.I., Weinhardt, V., Baumbach, T., Chaikina, M.V., Surmeneva, M.A., Surmenev, R.A., 2019. In vitro degradation behaviour of hybrid electrospun scaffolds of polycaprolactone and strontium-containing hydroxyapatite microparticles. Polym. Degrad. Stab. 167, 21–32.

Murugan, N., Murugan, C., Sundramoorthy, A.K., 2018. In vitro and in vivo characterization of mineralized hydroxyapatite/polycaprolactone-graphene oxide based bioactive multifunctional coating on Ti alloy for bone implant applications. Arab. J. Chem. 11, 959–969.

Reddy, S.H.R., Reddy, R., Babu, N.C., Ashok, G.N., 2018. Stem-cell therapy and platelet-rich plasma in regenerative medicines: a review on pros and cons of the technologies. J. Oral Maxill. Pathol.: JOMFP 22, 367.

Ramirez, G.A., Manfredi, A.A., Maugeri, N., 2019. Misunderstandings between platelets and neutrophils build in chronic inflammation. Front. Immunol. 10, 2491.

Sarkar, R., Agrawal, A., Ghosh, R., 2019. Preparation of ex-situ mixed sintered biphasic calcium phosphate ceramics from its co-precipitated precursors and their characterization. Trans. Indian Ceram. Soc. 78, 101–107.

Sarkar, M.R., Augat, P., Shefelbine, S.J., Schorlemmer, S., Huber-Lang, M., Claes, L., Kinzl, L., Ignatius, A., 2006. Bone formation in a long bone defect model using a platelet-rich plasma-loaded collagen scaffold. Biomaterials 27, 1817–1823.

Sadeghinia, A., Davaran, S., Salehi, R., Jamalpoor, Z., 2019. Nano-hydroxy apatite/chitosan/gelatin scaffolds enriched by a combination of platelet-rich plasma and fibrin glue enhance proliferation and differentiation of seeded human dental pulp stem cells. Biomed. Pharmacother. 109, 1924–1931.

Shamaz, B.H., Anitha, A., Vijayamohan, M., Kuttappan, S., Nair, S., Nair, M.B., 2015. Relevance of fiber integrated gelatin-nanohydroxyapatite composite scaffold for bone tissue regeneration. Nanotechnology 26, 405101.

Siddiqui, N., Madala, S., Parcha, S.R., Mallick, S.P., 2020. Osteogenic differentiation ability of human mesenchymal stem cells on Chitosan/Poly (Caprolactone)/nano beta Tricalcium Phosphate composite scaffolds. Biomed. Phys. Eng. Express 6, 015018.

Smith, R., Kaszniak, A.W., Katsanis, J., Lane, R.D., Nielsen, L., 2019. The importance of identifying underlying process abnormalities in alexithymia: Implications of the three-process model and a single case study illustration. Conscious. Cogn. 68, 33–46.

Subramanian, R., Sathish, S., Murugan, P., Musthafa, A.M., Elango, M., 2019. Effect of piperine on size, shape and morphology of hydroxyapatite nanoparticles synthesized by the chemical precipitation method. J. King Saud Univ.-Sci. 31, 667–673.

Shakir, M., Mirza, S., Jolly, R., Rauf, A., Owais, M., 2018. Synthesis, characterization and in vitro screening of a nano-hydroxyapatite/chitosan/Euryale ferox nanoensemble–an inimitable approach for bone tissue engineering. New J. Chem. 42, 363–371.

Skwarcz, S., Bryzek, I., Gregosiewicz, A., Warda, E., Gawęda, K., Tarczyńska, M., Skwarcz, J., Nadulski, R., Starek, A., Sanford, J., 2019. The effect of activated platelet-rich plasma (PRP) on tricalcium hydroxyapatite phosphate healing in experimental, partial defects of long bone shafts in animal models. Polish J. Veter. Sci., 243–250

Surmenev, R.A., Shkarina, S., Syromotina, D.S., Melnik, E.V., Shkarin, R., Selezneva, I.I., Ermakov, A.M., Ivlev, S.I., Cecilia, A., Weinhardt, V., Baumbach, T., 2019. Characterization of biomimetic silicate-and strontium-containing hydroxyapatite microparticles embedded in biodegradable electrospun polycaprolactone scaffolds for bone regeneration. Eur. Polym. J. 113, 67–77.

Shkarina, S., Shkarin, R., Weinhardt, V., Melnik, E., Vacun, G., Kluger, P.J., Loza, K., Epple, M., Ivlev, S.I., Baumbach, T., Surmeneva, M.A., 2018. 3D biodegradable scaffolds of polycaprolactone with silicate-containing hydroxyapatite microparticles for bone tissue engineering: High-resolution tomography and in vitro study. Sci. Rep. 8, 1–13.

Tang, Y., Zhang, H., Wei, Q., Tang, X., Zhuang, W., 2019. Biocompatible chitosan–collagen–hydroxyapatite nanofibers coated with platelet-rich plasma for regenerative engineering of the rotator cuff of the shoulder. RSC Adv. 9 (46), 27013–27020.

Tayapongsak, P., O'Brien, D.A., Monteiro, C.B., Arceo-Diaz, L.Y., 1994. Autologous fibrin adhesive in mandibular reconstruction with particulate cancellous bone and marrow. J. Oral Maxillofac. Surg. 52, 161–165.

Tian, G., Zhu, G., Xu, S., Ren, T., 2019. A novel shape memory poly (ε-caprolactone)/hydroxyapatite nanoparticle networks for potential biomedical applications. J. Solid State Chem. 272, 78–86.

Viswanathan, N., Kumar, I.A., Meenakshi, S., 2019. Development of chitosan encapsulated tricalcium phosphate biocomposite for fluoride retention. Int. J. Biol. Macromol. 133, 811–816.

Ventura, R.D., Padalhin, A.R., Lee, B.T., 2020. Functionalization of extracellular matrix (ECM) on multichannel biphasic calcium phosphate (BCP) granules for improved bone regeneration. Mater. Des. 108653.

Venkatesan, J., Kim, S.K., 2010. Effect of temperature on isolation and characterization of hydroxyapatite from tuna (Thunnus obesus) bone. Materials 3, 4761–4772.

Wright, Z.M., Arnold, A.M., Holt, B.D., Eckhart, K.E., Sydlik, S.A., 2019. Functional graphenic materials, graphene oxide, and graphene as scaffolds for bone regeneration. Regener. Eng. Transl. Med. 5, 190–209.

Wang, D., Jang, J., Kim, K., Kim, J., Park, C.B., 2019. "Tree to Bone": lignin/polycaprolactone nanofibers for hydroxyapatite biomineralization. Biomacromolecules 20, 2684–2693.

Wang, L., Fang, M., Xia, Y., Hou, J., Nan, X., Zhao, B., Wang, X., 2020. Preparation and biological properties of silk fibroin/nano-hydroxyapatite/graphene oxide scaffolds with an oriented channel-like structure. RSC Adv. 10, 10118–10128.

Xing, X., Cheng, G., Yin, C., Cheng, X., Cheng, Y., Ni, Y., Zhou, X., Deng, H., Li, Z., 2020. Magnesium-containing silk fibroin/polycaprolactone electrospun nanofibrous scaffolds for accelerating bone regeneration. Arab. J. Chem. 13, 5526–5538.

Zhou, D., Qi, C., Chen, Y.X., Zhu, Y.J., Sun, T.W., Chen, F., Zhang, C.Q., 2017. Comparative study of porous hydroxyapatite/chitosan and whitlockite/chitosan scaffolds for bone regeneration in calvarial defects. Int. J. Nanomed. 12, 2673.

Zheng, S., Guan, Y., Yu, H., Huang, G., Zheng, C., 2019. Poly-l-lysine-coated PLGA/poly (amino acid)-modified hydroxyapatite porous scaffolds as efficient tissue engineering scaffolds for cell adhesion, proliferation, and differentiation. New J. Chem. 43, 9989–10002.